Molecular Cancer Therapeutics

Bone-Seeking Matrix Metalloproteinase-2 Inhibitors Prevent Bone Metastatic Breast Cancer Growth

Marilena Tauro[1], Gemma Shay[1], Samer S. Sansil[2], Antonio Laghezza[3], Paolo Tortorella[3], Anthony M. Neuger[2], Hatem Soliman[4], and Conor C. Lynch[1]

Abstract

Bone metastasis is common during breast cancer progression. Matrix metalloproteinase-2 (MMP-2) is significantly associated with aggressive breast cancer and poorer overall survival. In bone, tumor- or host-derived MMP-2 contributes to breast cancer growth and does so by processing substrates, including type I collagen and TGFβ latency proteins. These data provide strong rationale for the application of MMP-2 inhibitors to treat the disease. However, *in vivo*, MMP-2 is systemically expressed. Therefore, to overcome potential toxicities noted with previous broad-spectrum MMP inhibitors (MMPIs), we used highly selective bisphosphonic-based MMP-2 inhibitors (BMMPIs) that allowed for specific bone targeting. *In vitro*, BMMPIs affected the viability of breast cancer cell lines and osteoclast precursors, but not osteoblasts. *In vivo*, we demonstrated using two bone metastatic models (PyMT-R221A and 4T1) that BMMPI treatment significantly reduced tumor growth and tumor-associated bone destruction. In addition, BMMPIs are superior in promoting tumor apoptosis compared with the standard-of-care bisphosphonate, zoledronate. We demonstrated MMP-2–selective inhibition in the bone microenvironment using specific and broad-spectrum MMP probes. Furthermore, compared with zoledronate, BMMPI-treated mice had significantly lower levels of TGFβ signaling and MMP-generated type I collagen carboxy-terminal fragments. Taken together, our data show the feasibility of selective inhibition of MMPs in the bone metastatic breast cancer microenvironment. We posit that BMMPIs could be easily translated to the clinical setting for the treatment of bone metastases given the well-tolerated nature of bisphosphonates. *Mol Cancer Ther; 1–12. ©2017 AACR.*

Introduction

Studies have shown that upon autopsy over 80% of women that succumb to breast cancer will have evidence of bone metastases (1). The metastases generate extensive bone destruction as a result of uncontrolled osteoclast activity that in turn cause the patient great pain and contribute significantly to the morbidity associated with the disease. Tumor–bone interaction has been classically described as a "vicious cycle" in which breast cancer cells promote the expression of potent osteoclastogenic factors such as receptor activator of nuclear kappa B ligand (RANKL) by bone-lining osteoblasts (2). Upon exposure to RANKL and other osteoclastogenic factors, myeloid-derived osteoclast precursors fuse to form multinucleated osteoclasts that resorb the mineralized matrix and release growth factors, such as TGFβ that in turn drives cancer cell growth and completes the vicious cycle (3). As the metastases are dependent on the surrounding bone microenvironment to grow, it is logical that targeted therapies preventing cancer–bone stroma cross-talk would be of therapeutic value. To this end, bisphosphonates, such as zoledronate, have been used for treatment of patients with bone metastases (4). Bisphosphonates home the skeletal tissue and bind to hydroxyapatite via their bisphosphonic moiety (5). During osteoclast-mediated resorption, bisphosphonate internalization causes osteoclast apoptosis via mechanisms including the inhibition of enzymes critical for metabolism such as farnesyl pyrophosphate (FPP) synthase and ATP analogue formation (6). However, while bisphosphonates delay the time to first skeletal-related event (SRE) such as pathologic fracture, they do not significantly extend overall survival for the majority of patients with bone metastases (7, 8). Other microenvironmental-targeted therapies, such as RANKL-based inhibitors and radium-223, have improved time to first SRE and overall survival for patients with bone metastatic disease, respectively (9). Thus, there is strong rationale for further definition of the molecular circuitry underpinning cancer–bone communication so as to generate new therapies that can cure the disease or significantly improve overall survival rates. In this regard, previous work from our group and others has highlighted the role of individual matrix metalloproteinases (MMP) such as MMP-2, 7, 9, 13, and 14 in controlling cancer–bone interaction (10).

MMPs process extracellular matrix (ECM) but also play key roles in regulating the bioavailability/activity of growth factors and cytokines (10). For example, host- and tumor-derived MMP-2 significantly contributes to bone metastatic breast cancer progression by processing matrix and nonmatrix factors including, but not limited to, type I collagen and TGFβ latency–binding proteins

[1]Tumor Biology Department, H. Lee Moffitt Cancer Center and Research Institute, Tampa, Florida. [2]Translational Research Core and, H. Lee Moffitt Cancer Center and Research Institute, Tampa, Florida. [3]Department of Pharmacy-Pharmaceutical Sciences, University of Bari "A. Moro", Bari, Italy. [4]Department of Women's Oncology and Experimental Therapeutics, H. Lee Moffitt Cancer Center and Research Institute, Tampa, Florida.

Note: Supplementary data for this article are available at Molecular Cancer Therapeutics Online (http://mct.aacrjournals.org/).

Corresponding Author: Conor C. Lynch, Tumor Biology Department, H. Lee Moffitt Cancer Center and Research Institute, SRB-3, 12902 Magnolia Drive, Tampa, FL 33612. Phone: 813-745-8094; Fax: 813-745-3829; E-mail: conor.lynch@moffitt.org

doi: 10.1158/1535-7163.MCT-16-0315-T

(11–14). These data provide rationale for the application of MMP inhibitors for the treatment of bone metastatic disease. However, enthusiasm for MMPIs in the clinical setting has been dampened by the results of unsuccessful trials performed with broad-spectrum inhibitors over two decades ago (15). The reasons for the failure of the clinical trials are several fold including dose-limiting toxicity and the lack of knowledge pertaining to nonmatrix MMP substrates (16). Subsequent studies have therefore focused on defining individual MMPs that contribute to cancer progression to identify the "bad actors" and generate highly specific targeted inhibitors. Because of data pointing to a role for MMP-2 in driving bone metastatic breast cancer survival and growth, we hypothesized that selective MMP-2 inhibition would be an effective strategy for treatment of the disease. However, given the systemic expression of the enzyme, off-target effects and dose-limiting toxicities would be a potential concern (17). To combat this, we describe herein a strategy for inhibiting MMP-2 in the skeletal tissue by using bisphosphonic-based highly selective MMP-2 inhibitors (18, 19). Using these novel bone-seeking MMPI (BMMPI) compounds, we demonstrate that metastatic breast cancer growth in bone can be prevented *in vivo* and that specific tissue inhibition of MMP-2 is feasible.

Materials and Methods

Public database analyses

The Molecular Cancer Therapeutics for Ireland (MCTI, http://glados.ucd.ie/BreastMark/) and The Cancer Genome Atlas (TCGA, http://tcga-data.nci.nih.gov) portals were used to examine the expression of MMP-2 in breast cancer basal like subtypes (20, 21). High (top 25% expression level) and low (bottom 25% expression level) cutoffs were determined by the databases. Km plotter (http://kmplot.com/analysis) was used to generate survival analyses.

Cell lines and culture

Human breast cancer cell lines were obtained in 2003 from the ATCC (MDA-MB-231, T47) or collaborators in 2014 (MDA-4175 and 1833) and undergo short tandem repeat testing (STR) at the Moffitt Genomics Core every 10 passages to ensure authenticity. Murine mammary cancer cell lines (PyMT-R221A and 4T1) were obtained from collaborators in 2004 and undergo evaluation for interspecies contamination and mouse STR (Idexx). All cell lines used in this study have been validated within the last 6 months. PyMT, 4T1, and the human breast cancer MDA-MB-231 parental and metastatic variants (4175 and 1833) were all cultured in DMEM supplemented with 10% FBS with the exception that MDA series received 1% glutamine. The human T47D breast cancer cell line was grown in 10% serum containing RPMI. MC3T3-E1 and RAW264.7 cells were grown in αMEM with 10% FBS. All cell lines were periodically tested for mycoplasma (#CUL001B, R&D Systems). Primary monocytic cells were isolated freshly using cd11b magnetic beads (130-049-601, Miltenyi Biotec) as per manufacturer's instructions. Isolated cells were grown in αMEM with 10% FBS expanded with 20 ng/mL of macrophage-colony stimulating factor (M-CSF; 315-02, PeproTech) to generate sufficient cell numbers for subsequent assays.

Zymography

For analysis of MMP-2 enzymatic activity, conditioned media from cell lines was normalized for total protein using a BCA (bicinchoninic acid assay) kit (#23225, Pierce). For gelatin zymography, gelatin was added to SDS-resolving gels to a final concentration of 1 mg/mL and equal amounts of total protein (30 μg/well) were run under nonreducing conditions. After electrophoresis, the gels were washed in 2.5% solution of Triton-X-100 followed by overnight incubation at 37°C in substrate buffer (50 mmol/L Tris-HCL, pH 7.4, containing 5 mmol/L $CaCl_2$). The following day, the gels were stained with a 5 mg/mL Coomassie brilliant blue solution (1 part acetic acid: 3 parts isopropyl alcohol: 6 parts water) and then destained in water and digitized.

Hydroxyapatite affinity measurement

A solution of each BMMPI reagent (ML104, ML111, and ML115) and tiludronate (100 μmol/L) in Tris-HCl buffer (50 mmol/L, pH 7.5) was mixed with hydroxyapatite (HAP, 0.8 mg/mL) and stirred at 37°C. After 2 hours, the mixtures were centrifuged (10 minutes, 10,000 × *g*), supernatants were syringe-filtered (0.22 μm), and the absorbance was measured with UV-VIS spectrometer (18). Using a UV calibration curve for each compound, the percentage of HAP binding was determined. The resulting λ-max, ε-value, angular coefficient of the calibration curve (m), and the coefficient of determination (R^2) related are listed in Supplementary Table S1.

In vitro analyses

Cell lines were plated in 96-well plates at a density of 5×10^3 and allowed to incubate overnight. The following day, cells were treated with vehicle or a range of inhibitors (10^{-8} to 10^{-4} mol/L). Cell viability was measured at 48 hours via MTT assay (Cell Titer 96-Sigma Aldrich), as per manufacturer's instructions. The absorbance was measured at 490 nm using a Perkin Elmer VictorV3 plate reader. IC_{50} values were determined from dose–response curves using GraphPad PRISM version 6.0 as described previously (18). MMP-2 and 9 inhibition assays with the BMMPI compounds were performed as described previously (18). For TGFβ treatment, cells were set up in a similar manner and then treated in the presence or absence of BMMPI with 1 ng/mL of recombinant TGFβ.

In vivo studies

All animal experiments were performed with Institutional Animal Care and Use Committee (IACUC) approval (#IS00000027, CCL) from the University of South Florida. To test the efficacy of BMMPIs *in vivo*, immunocompromised RAG-2 mice were intratibially inoculated with 1×10^5 (10-μL volume in ice-cold PBS) luciferase-expressing PyMT-Luc or 4T1-Luc cells (11). After 3 days, mice ($n \geq 7$/group) were treated in the following manner for high dose studies; vehicle (PBS); ML104, (25 mg/kg); ML115 (25 mg/kg); tiludronate (25 mg/kg, synthesized by M. Tauro and P. Tortorella) and for low-dose studies; vehicle (PBS), ML115 (1 mg/kg) and, zoledronate (1 mg/kg, #SML0223, Sigma-Aldrich). Vehicle and treatment reagents were given via subcutaneous injection (0.1 cc) three times a week. Bioluminescence (120 mg/kg luciferin in sterile PBS, LUCK-1G, Gold Biotechnology) was measured every two days as a correlate of tumor growth (IVIS Perkin Elmer). We chose a range between day 8 and 13 as the clinical endpoint for our studies with both the PyMT-Luc and 4T1-Luc models. At this time-point, the cancer cells compromise the cortical bone and begin growing in the surrounding soft tissue (11, 22, 23). At the clinical endpoint, serum was

collected from each of the animals via cardiac puncture. The tumor-bearing and sham-bearing legs were collected and either flushed for collection of bone marrow supernatant or fixed in formalin overnight before being transferred to 70% ethanol for *ex vivo* analysis. Subsequent to *ex vivo* analyses, bones were decalcified (14% EDTA, pH 7.4 over three weeks) and dehydrated through ethanol/xylenes series prior to paraffin embedding.

For biodistribution studies, PyMT tumor–bearing mice were injected with a single subcutaneous dose of ML115 (5 mg/kg, $n = 3$/time-point) and peripheral blood drawn at 15, 30 minutes, 1, 2, 4, 8, and 24-hour time-points. Mice at each time point were euthanatized and bone marrow supernatants collected. Subsets of tumor-bearing mice (non-ML115–injected; $n = 3$/time point) served as baseline controls for all time point measurements. To determine the effect of ML115 accumulation in the bone, tumor-bearing mice were treated for three weeks (ML115 at 5 mg/kg, three times/week). On the final day of dosing, mice were euthanatized at the 15-minute or 24-hour time points. Peripheral blood and bone marrow supernatant was collected at each time point. Peripheral blood sampling was centrifuged to harvest plasma and all samples were frozen at −80°C prior to LC/MS-MS. To this end, plasma was combined with 1.2 N perchloric acid then vortexed and centrifuged. Bone marrow supernatant was treated similarly (24, 25). All samples were further diluted with HPLC water to reduce matrix interferences. Sample was injected into a Thermo Dionex UHPLC coupled to a Thermo TSQ Quantiva tandem mass spectrometer (Thermo Electron). Gradient elution was achieved with mobile phases of 10 mmol/L ammonium acetate and methanol, both containing 0.1% ammonium hydroxide. A Kinetex reverse phase C18 column (Phenomenex) was used to separate compounds in plasma while a Kinetex Biphenyl column was utilized for bone marrow supernatant. The mass spectrometry system employed heated electrospray ionization (H-ESI) in the source followed by selected reaction monitoring (SRM) of the target compound. The following SRM transition was monitored in negative ion mode for quantitation: 406.07 → 324.04 of ML115. The assay has a linear range from 5 to 2,500 ng/mL for plasma and from 50 to 2,500 ng/mL for bone marrow supernatant. Concentration–time data for ML115 was analyzed by noncompartmental methods using Phoenix WinNonlin 6.4 (Certara). Plasma data in the terminal, log-linear phase were analyzed by linear regression to estimate terminal elimination rate constant and half-life.

Microcomputed tomography and X-ray

For gross analysis of trabecular bone volume, formalin-fixed tibiae were scanned at an isotropic voxel size of 18 μm (Siemens Inveon PET/CT/SPECT scanner with cone beam X-Ray source). The scans were performed at 80 kVp voltage and 500 mA current with an exposition time of 3,000 ms per projection. The tissue volume (TV) was derived from generating a contour around the metaphyseal trabecular bone that excluded the cortices. The area of measurement began at least 0.5 mm below the growth plate and was extended by 1.8 mm (100 × 8 μm slices). The bone volume (BV) included all bone tissue that had a material density greater than 438.7 mg HA/cm^3. These analyses allowed for the calculation of the BV/TV ratio. The threshold setting for bone tissue was determined on the basis of control sham tibia and was used for all samples. Radiographic images (Faxitron X-ray Corp) were obtained using an energy of 35 kVp and an exposure time of 8 ms. The spatial resolution was 10 lp/mm (48 μm). The tumor volume (TuV) was calculated as a function of the total tissue volume (TV) of the tibial medullary canal using ImageJ software (26).

Immunohistochemistry and histology

Sections (5-μm thick) were rehydrated and blocked prior to the addition of specific primary antibody (cleaved caspase-3, #9964S, Cell Signaling Technology; phospho-Histone H3, #04-1093, Millipore; pSMAD2, #AB3849, Millipore) and appropriate IgG controls. Tissue sections were incubated overnight at 4°C. Subsequently, species-specific secondary AlexaFluor 568 antibodies (1: 1,000 dilution for 1 hour at room temperature; #A10042 and #A21202, Invitrogen) were added for imaging by microscopy. For quantitation of bone volume, mouse tibiae were stained with Trichrome stain. Tartrate-resistant acid phosphatase (TRAcP), a marker of mature osteoclasts, was detected using a colorimetric kit according to the manufacturer's instructions (Kit 387-A, Sigma-Aldrich). Sections were scanned and quantified using Definiens tissue studio software and ImageJ.

MMP activity assays

At the study endpoint, serum and supernatants from bone marrow flushes of tumor-bearing limbs were collected from each group for *ex vivo* MMP enzymatic assays. Samples were kept at 4°C to avoid freeze–thaw activation of latent MMPs. Prior to assaying for MMP activity, samples were normalized for total protein via BCA assay (#23225, Pierce). MMP-2 and MMP-13 activity levels were measured (20 μL/serum or bone marrow sample final volume) using specific fluorogenic peptides according to manufacturer's instructions (MMP-2; #032014-01, MMP-13; #032014-11, EnSens). As a positive control, bone marrow flushes and serum from control groups were pretreated with GM6001 (10 μmol/L final concentration of broad spectrum MMP inhibitor, #CC1010, Millipore) for 1 hour at room temperature. Fluorescence was read at Ex/Em 625–635 nm/655–665 nm. For total MMP activity, we used a broad-spectrum fluorogenic substrate (OMNI-MMP, #BML-P126-0001, Enzo Life Sciences) according to the manufacturer's instructions. Sample set up was similar to that described for MMP-2. Fluorescence was read at Ex 320 nm/Em 405 nm. All reactions were performed in triplicate. To compare outputs between probes, the percentage relative activity (%RA) was calculated as follows: % RA = RFU sample/RFU control × 100.

For ICTP ELISA (MyBioSource, #MBS030383), bone marrow supernatants were normalized and assayed according to the manufacturer's instructions.

Statistical analyses

Statistical analyses were performed using Student t test or ANOVA where appropriate using GraphPad Prism (GraphPad Software, Inc). Data are presented as mean ± SD.

Results

MMP-2 is associated with aggressive breast cancer

High expression of MMP-2 has been classically associated with aggressive forms of breast cancer and has been demonstrated to be a poor prognostic indicator for overall survival (27–30). Our interrogation of independent publicly available datasets also illustrates that high expression of MMP-2 is significantly

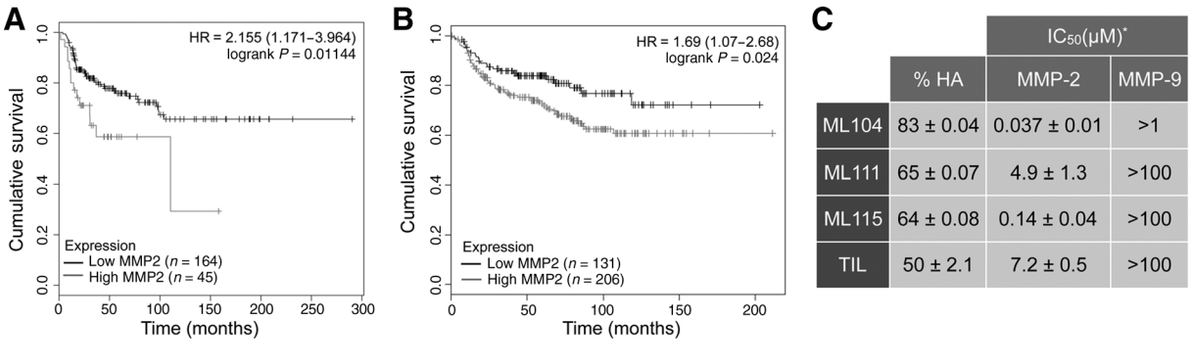

C

	% HA	$IC_{50}(\mu M)^*$ MMP-2	MMP-9
ML104	83 ± 0.04	0.037 ± 0.01	>1
ML111	65 ± 0.07	4.9 ± 1.3	>100
ML115	64 ± 0.08	0.14 ± 0.04	>100
TIL	50 ± 2.1	7.2 ± 0.5	>100

Figure 1.

High expression of MMP-2 correlates with aggressive and advanced tumor stage in breast cancer. **A** and **B,** Distant disease-free survival data from Breast Mark (**A**) and TCGA (**B**) databases were used to generate Kaplan–Meier survival curves for patients with high (gray line) or low (black line) expression of MMP-2. *P* values were determined by the Mantel–Cox log-rank test. **C,** Characteristics of BMMPIs (ML104, ML111, and ML115) and tiludronate for binding to hydroxyapatite (%HA). IC_{50} for each compound against recombinant active MMP-2 and MMP-9 are displayed. Asterisk denotes data adapted from Rubino et al. (18).

associated with aggressive disease (Fig. 1A and B). Underscoring this observation is the fact that murine and human metastatic cell lines generate varying levels of active MMP-2 (Supplementary Fig. S1A). Breast cancer commonly metastasizes to the bone and work from our group and others has highlighted the contributory role of tumor and host-derived MMP-2 to the progression of bone metastatic disease (11, 12). Because previous iterations of MMP inhibitors had systemic dose-limiting issues, we chose a strategy of selectively targeting the bone microenvironment by using a bisphosphonic moiety as a foundation. With this approach, a panel of tiludronate-based MMP-2 inhibitors that could essentially seek out and "stick" to skeletal tissue were developed (Supplementary Fig. S1B). Of the inhibitors synthesized, ML104 and ML115 inhibit MMP-2 in the nanomolar range without inhibiting other closely related family members and further retain their ability to bind hydroxyapatite (Fig. 1C; Supplementary Fig. S2; ref. 18). As a control, we included ML111 that binds hydroxyapatite but poorly inhibits MMP-2 in comparison with ML104 and ML115 (Fig. 1C).

BMMPIs directly limit cancer cell and osteoclast precursor viability

Next, we tested the effect of the BMMPI reagents on the viability of breast cancer and bone stromal cell lines. In murine and human breast cancer cell lines, results indicate differing levels of sensitivity to the MMP-2–specific ML104 and ML115 BMMPIs with IC_{50} values in the nanomolar to the micromolar range (Fig. 2A: ML104; 4T1 = 0.93 μmol/L, PyMT-R221A = 38.6 μmol/L, T47D = 48 μmol/L, MDA-1833 >100 μmol/L and ML115; 4T1 = 0.18 μmol/L, PyMT-R221A = 40 μmol/L, T47D >100 μmol/L, MDA-1833 >100 μmol/L). IC_{50} values for the MMP-2 nonspecific compounds, ML111 and tiludronate, were >100 μmol/L for all cancer cell lines tested. RAW 264.7 and $CD11b^+$ isolated cells from the bone marrow are monocytic cells that can be differentiated into osteoclasts. BMMPI treatment of these osteoclast precursor cultures revealed IC_{50} values in the micromolar range (ML104; RAW 264.7 = 29.2 μmol/L, cd11b = 29.1 μmol/L and ML115; RAW 264.7 = 5.6 μmol/L, cd11b = 41 μmol/L). In contrast, ML111 had IC_{50} values >100 μmol/L while tiludronate had IC_{50} values of >100 μmol/L and 6.5 μmol/L for the RAW 264.7 and $CD11b^+$ cells, respectively. (Fig. 2B). We also tested the effect of the BMMPIs and tiludronate on osteoblast viability using the same dose range. We found that none of the compounds impacted osteoblast viability, even at concentrations >100 μmol/L (Fig. 2C). However, at lower concentrations (nanomolar range), we noticed that the BMMPIs promoted osteoblast growth. While we did not observe this phenomenon with tiludronate, a low-dose proliferative effect on osteoblasts has been noted for other bisphosphonates (31).

BMMPIs prevent breast cancer growth and associated bone destruction *in vivo*

To determine the *in vivo* efficacy of the inhibitors, the tibias of immunocompromised RAG-2 animals were intratibially inoculated with PyMT-R221A luciferase–expressing cells that grow in the bone microenvironment and induce rapid osteolytic lesions (11, 22). On the basis of tiludronate dosing and frequency in the literature, we treated the animals (upon establishment of the tumors) with vehicle, ML104, ML115, and tiludronate (n = 7/group) at a concentration of 25 mg/kg subcutaneously every three days (32–34). We did not include ML111 given the similar performance of this BMMPI to tiludronate *in vitro*. Using bioluminescence as a readout, we calculated the individual growth rate of the tumors in each of the groups. Analysis of the average growth rate identified that the MMP-2–specific BMMPIs, ML115 and ML104, were superior to tiludronate in limiting the growth of the PyMT-R221A cells in the bone microenvironment (Fig. 3A). Measurement of osteolytic lesions by X-ray analysis also demonstrated that ML104 and ML115 were comparable with tiludronate in protecting against tumor-induced osteolysis with greater than 50% decrease compared with control groups noted for each compound (Fig. 3B). To validate the robustness of this observation, we repeated the study with 4T1 luciferase-expressing cells. We used RAG-2–null mice to directly compare 4T1 results to those obtained with the PyMT-R221A model. Again, using an intratibial approach, we found that ML115 significantly reduced the growth of 4T1 and the extent of tumor-induced osteolysis *in vivo* compared with vehicle control (Supplementary Fig. S3). These data indicate that the BMMPIs work by limiting tumor growth and protecting against cancer-induced bone loss and also define ML115 as the lead BMMPI compound for the treatment of breast cancer in bone.

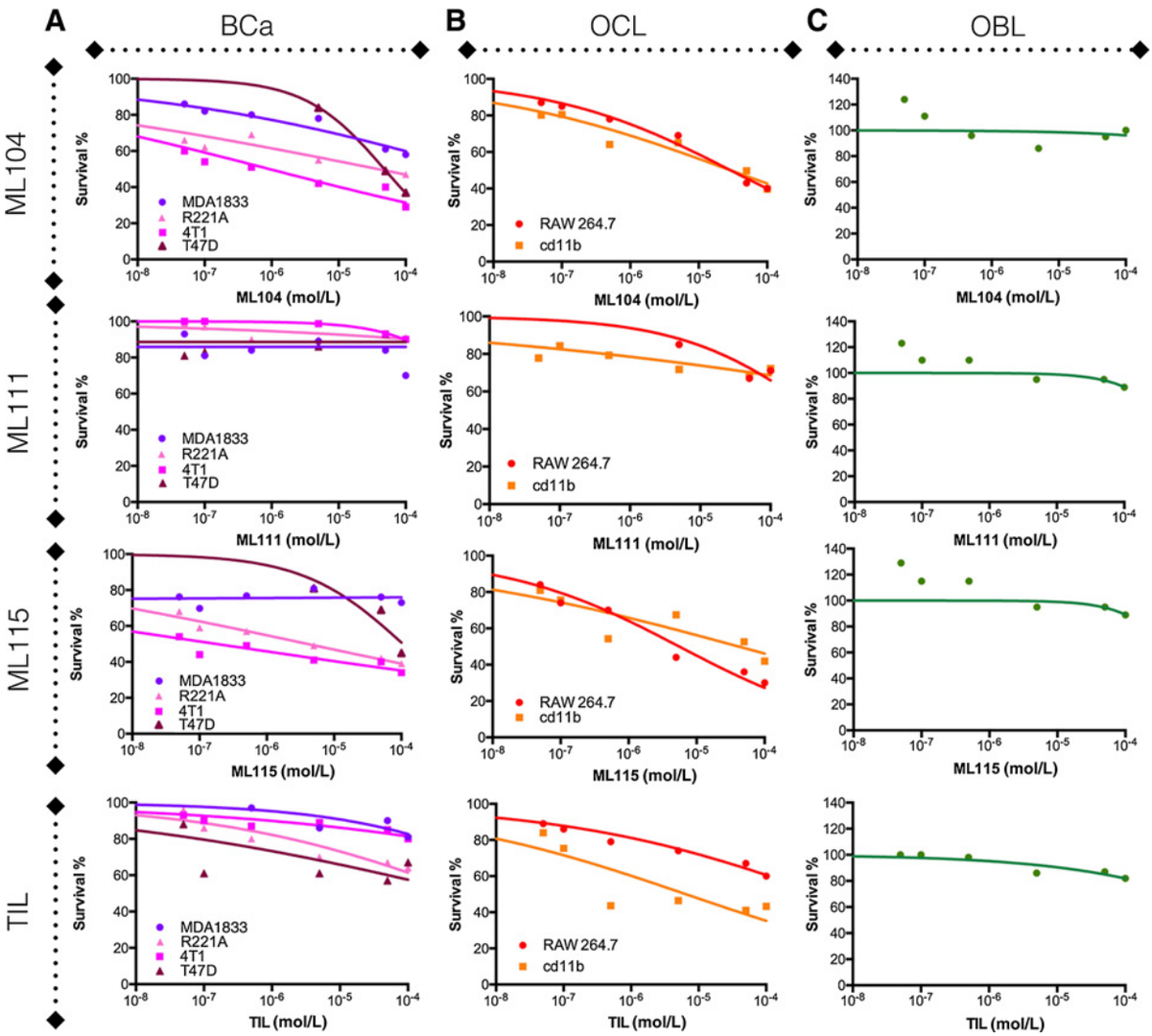

Figure 2.

BMMPI effects on the cellular components of the vicious cycle. **A–C,** The bone metastatic variant of MDA-MB-231 (MDA1833), T47D, and murine mammary cancer cell lines 4T1 and PyMT-R221A (**A**), RAW 264.7 and cd11b-selected primary monocytic cell lines (**B**), and the osteoblast precursor cell line, MC3T3-E1 (**C**), were treated with varying concentrations of the BMMPIs ML104, ML111, ML115 and, the bisphosphonate, tiludronate (10^{-8} to 10^{-4} mol/L for all compounds), for 48 hours. Survival values derived from MTT assay are calculated as a percentage of the control group.

BMMPIs are as effective as zoledronate *in vivo*

Currently, the "gold-standard" bisphosphonate for the treatment of skeletal metastases is zoledronate. Zoledronate is highly effective at limiting cancer-induced bone destruction and significantly prevents time to first SRE (6). We therefore compared the efficacy of the BMMPI, ML115, to that of zoledronate. Similarly, to tiludronate, zoledronate has inherent MMP activity but the IC_{50} for MMP-2 is in the micromolar range and 50-fold higher than that of ML115 (Supplementary Fig. S2; ref. 18). Mice ($n = 7$/group) were intratibially inoculated with PyMT-R221A cells and treated with vehicle alone, ML115, or zoledronate. In this *in vivo* study, we used a concentration of ML115 that was comparable with the clinical dose of zoledronate (1 mg/kg) and administered the reagents three times a week subcutaneously (35). Data analysis shows that ML115 significantly prevents the growth of bone metastatic breast cancer compared with the vehicle control group and the ML115 median growth rate trended lower than that of the zoledronate-treated group (Fig. 4A). X-ray analysis of cancer-induced osteolysis also revealed that ML115 was as effective as zoledronate in mitigating bone destruction (Fig. 4B). Using high-resolution μCT, we examined the protective effect of ML115 on the trabecular bone architecture in tumor-bearing tibias. Our analyses show that ML115 prevented cancer-induced bone loss compared with the control group (BV:TV: control = 0.36 vs. ML115 = 0.61) and performed as well as zoledronate (Fig. 4C). Histomorphometry analyses confirm X-ray and μCT analyses and demonstrate the bone-protective effect of ML115 (Fig. 5A). We also found that ML115 significantly decreased the number of TRAcP-positive osteoclasts/mm of bone interface compared with the control group and to a similar extent to that of the

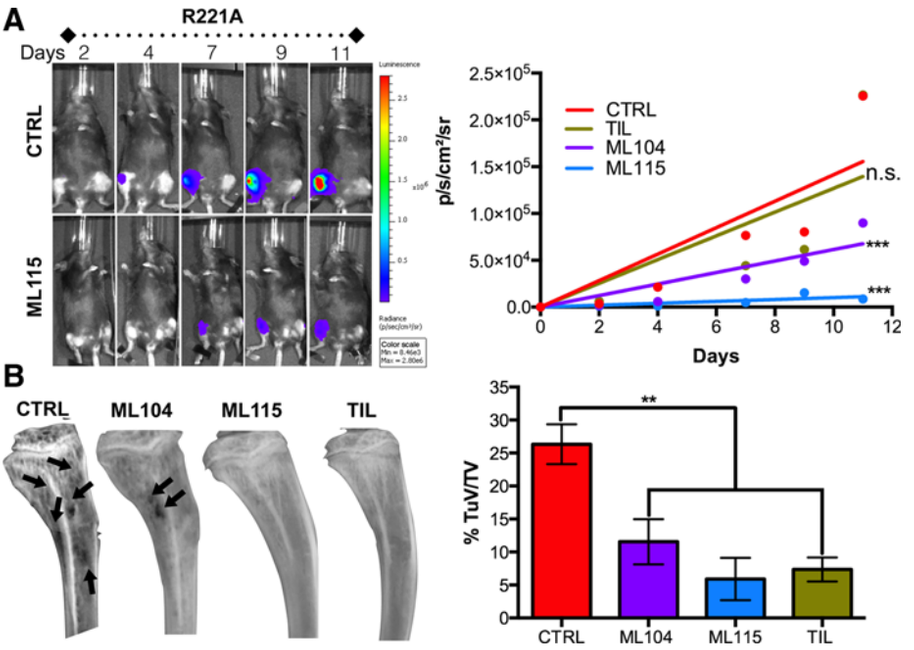

Figure 3.
Impact of BMMPIs on bone metastatic breast cancer growth and osteolysis. **A,** RAG-2–null females ($n = 7$/group) were inoculated with PyMT-R221A luciferase–expressing cells and bioluminescence, as a correlate of tumor growth, was measured over time. Mice were treated with PBS vehicle (CTRL), tiludronate (TIL) as a positive control or, the BMMPIs ML104 or ML115 (25 mg/kg), three times per week for the duration of the study. The median growth rate (slope of the line for each animal) was subsequently calculated and averaged. Representative longitudinal images from the vehicle control (CTRL) and ML115 groups are shown. **B,** X-ray analysis of tumor-bearing tibias identified areas of cancer-induced osteolysis (arrows). The tumor volume (TuV) as a ratio of the total volume (TV) was measured for each animal/group. Asterisks denote statistical significance (**, $P < 0.01$; ***, $P < 0.001$).

zoledronate-treated group (Fig. 5B). Phospho-histone-H3 staining revealed a significant decrease in proliferation in the ML115- and zoledronate-treated groups (Fig. 5C). However, using cleaved caspase-3 as a readout for apoptosis, we observed a significant increase in the number of apoptotic cells in the ML115 group compared with the control and zoledronate-treated groups, potentially explaining the enhanced effect of ML115 in limiting tumor growth in bone (Fig. 5D).

BMMPIs selectively inhibit MMP-2 activity in the tumor–bone microenvironment

To ensure that ML115 was reaching the bone marrow microenvironment, we conducted biodistribution studies in tumor-bearing animals. Using LC/MS-MS approaches, we identified that ML115 concentration peaks in the plasma within 15 minutes after subcutaneous injection and that levels rapidly return to baseline within 1 hour (Supplementary Fig. S4). Conversely, and expected given the bisphosphonic nature of ML115, we observed a steady increase in concentration over a 24-hour period in the bone marrow microenvironment. We also observed that the concentration of ML115 in the bone marrow microenvironment in mice treated for a 3-week period was 10-fold higher than that compared with mice that received a single dose of ML115 over a 24-hour period (Supplementary Fig. S4).

Next, to determine whether MMP-2 was being specifically inhibited in the breast cancer–bone microenvironment, we used MMP-2–specific and broad-spectrum MMP-activatable fluorescent probes. We also included a specific probe for MMP-13, a type I collagenase, whose expression is largely restricted to skeletal tissue. Serum and bone marrow flushes from vehicle control, ML115, and zoledronate-treated animals were collected at experimental endpoints ($n \geq 3$/group), normalized for total protein and tumor burden. Our data show that MMP-2 activity was significantly lower in the ML115-treated mice compared with either control or zoledronate groups (Fig. 6A). MMP-13 activity was also unaffected compared with control although we did note interestingly that MMP-13 activity levels were significantly lower in the zoledronate group (Fig. 6B). As anticipated, ML115 did not affect broad-spectrum MMP activity (Fig. 6C). We also examined whether the inhibition of MMP-2 was systemic. Analysis of serum showed no difference in MMP-2 activity between the control, ML115, and zoledronate groups using any of the MMP probes (Fig. 6A–C).

BMMPIs limit the bioavailability of MMP-2 substrates in bone

MMP-2 is known to regulate the bioactivity and bioavailability of a range of growth factors and cytokines including, as we have previously reported, TGFβ (11, 14). We therefore examined phosphorylated SMAD2 (pSMAD2) levels as a correlate for TGFβ signaling activity and observed significantly less pSMAD2 in the ML115-treated mice compared with control and zoledronate-treated groups (Fig. 7A and B). Interestingly, the addition of recombinant TGFβ to breast cancer cell lines treated with an IC_{50} dose of ML115 rescued its inhibitory effect (Supplementary Fig. S5). We also examined other MMP-2 substrates. MMPs such as MMP-2 can generate ICTP fragments of type I collagen that are distinct from those generated by other type I collagenases such as cathepsin-K (36). Analysis of bone marrow supernatants by ELISA revealed significantly lower levels of ICTP in the ML115-treated mice compared with the control group (Fig. 7C). These data suggest that the decrease in bioavailable TGFβ and type I collagen degradation may, in part, be responsible for the increased apoptosis observed in the ML115-treated group. Collectively, our data show that MMP-2 can be specifically targeted in the bone tissue using the novel approach of grafting the inhibitor onto a bisphosphonic backbone and that the approach is effective at limiting the growth of breast to bone metastases.

Discussion

On the basis of the roles for MMP-2 in cancer and bone disease, we hypothesized that inhibition of MMP-2 would be effective for

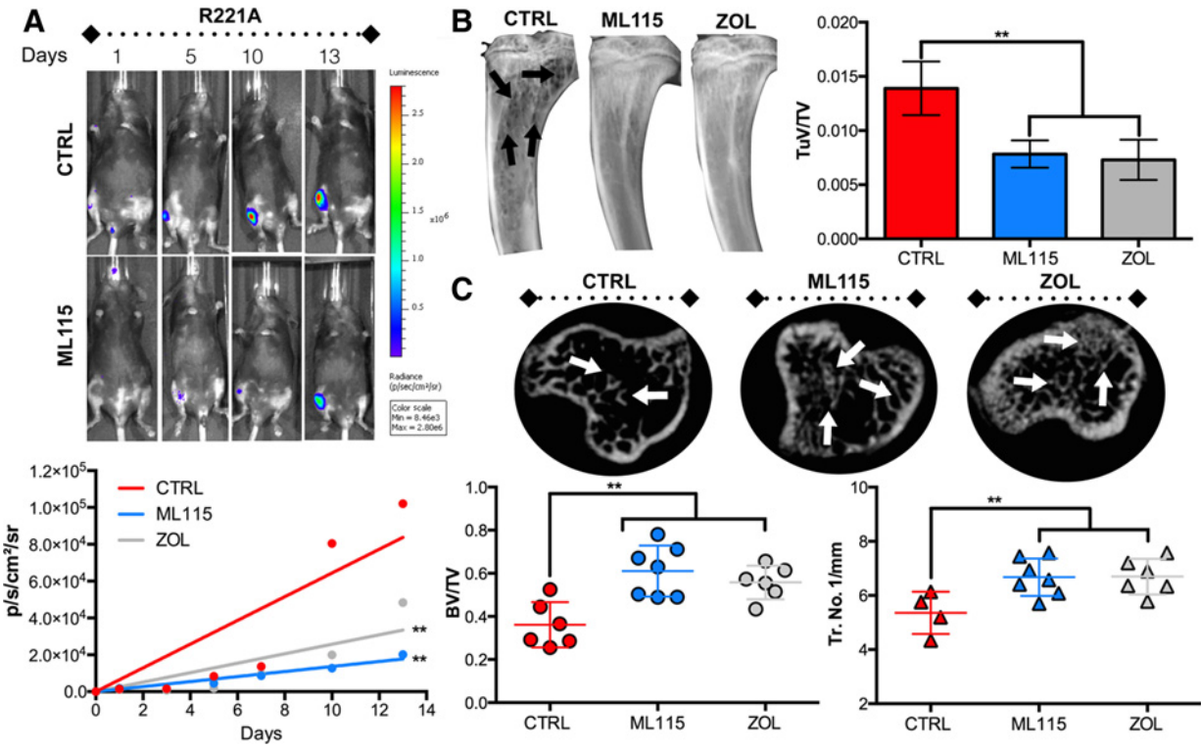

Figure 4.

Comparison of BMMPI efficacy to zoledronate. **A,** PyMT-R221A tumor growth (bioluminescence), was measured in the control (PBS, $n = 7$/group), ML115 (1 mg/kg, $n = 7$/group), and zoledronate (ZOL, 1 mg/kg, $n = 7$/group)-treated mice. Mice received treatments three times per week for the duration of the study. The median growth rate (slope of the line for each animal) was subsequently calculated and averaged. Representative longitudinal images from the vehicle control (CTRL) and ML115 groups are shown. **B,** The tumor volume (TuV; arrows) as a ratio of the total volume (TV) was measured for each animal/group. **C,** μCT scan analysis of the trabecular bone architecture (arrows) in the control, ML115, and zoledronate-treated groups. Bone volume (BV) was measured as ratio to total volume (TV). The trabecular number/mm (Tr. No./1 mm) was also determined. Asterisks denote statistical significance (**, $P < 0.01$).

the treatment of breast to bone metastases (11, 27–30). However, MMP-2 is expressed systemically suggesting that long-term inhibition could have potentially undesirable effects. To address this, we used novel BMMPI compounds that were bisphosphonic based and highly selective for MMP-2 thereby allowing the specific targeting of areas of bone turnover. Our data with two different animal models show that BMMPIs are effective in preventing cancer growth by presumably directly impacting cancer cell survival as suggested by IC_{50} data for 4T1, PyMT-R221A, and T47D. This raises the question as to whether the growth of BMMPI-resistant cell lines such as MDA-MB-1833 would be mitigated *in vivo*. Previously, we reported that ablation of MMP-2 from the host compartment significantly reduced tumor growth. Therefore, we posit that the BMMPI effect on osteoclast survival and the release of growth factors, such as TGFβ, would indirectly limit the growth of the MDA-MB-1833 cell line *in vivo* as well. BMMPIs also successfully limit cancer induced bone destruction when applied in a pretreatment manner using our intratibial approach. Bone fracture and pain are significant morbidities for women diagnosed with bone metastases and given their dual MMP inhibitory and bisphosphonic activity, we would predict BMMPIs would reduce time to SREs. Whether BMMPIs can extend overall survival in clinical trials or prevent seeding/establishment in the bone microenvironment remains to be determined. A caveat of our *in vivo* results is the use of immunocompromised RAG-2–null mice that lack mature B- and T-cells. The rationale for using RAG-2 mice was to directly compare results between the PyMT and 4T1 models. T cells can contribute and protect against cancer progression depending on their polarization state. Reports have demonstrated that bisphosphonates can facilitate the recruitment of cytotoxic γδ T cells and therefore we would predict that the BMMPI compounds would also be effective in immunocompetent models (37). The PyMT and 4T1 cell lines are syngeneic with FVB and BALB/c immunocompetent mice respectively, and thus the impact of BMMPIs in immunocompetent models of bone metastatic breast cancer can be addressed with these models.

Analysis of bone marrow and serum samples from tumor-bearing animals also demonstrates the selective inhibition of MMP-2 activity in bone tissue with the BMMPI, ML115, compared with control or zoledronate-treated samples. *In vivo*, we posit that the combined MMP-2 inhibitor and bisphosphonic activity of the BMMPIs can both directly and indirectly limit bone metastatic breast cancer cell growth (Fig. 7D). Bone is a dynamic tissue that is continually undergoing remodeling. While osteoclast-derived cathepsin-K is a key regulator of bone extracellular matrix turnover, MMPs, in particular those with the ability to cleave type-I collagen such as MMP-1, 2, 13, and 14 also play important roles in the process (38, 39). This is evidenced in large part from developmental studies where mice null for specific MMPs have either transient or sustained deficiencies in skeletal development and

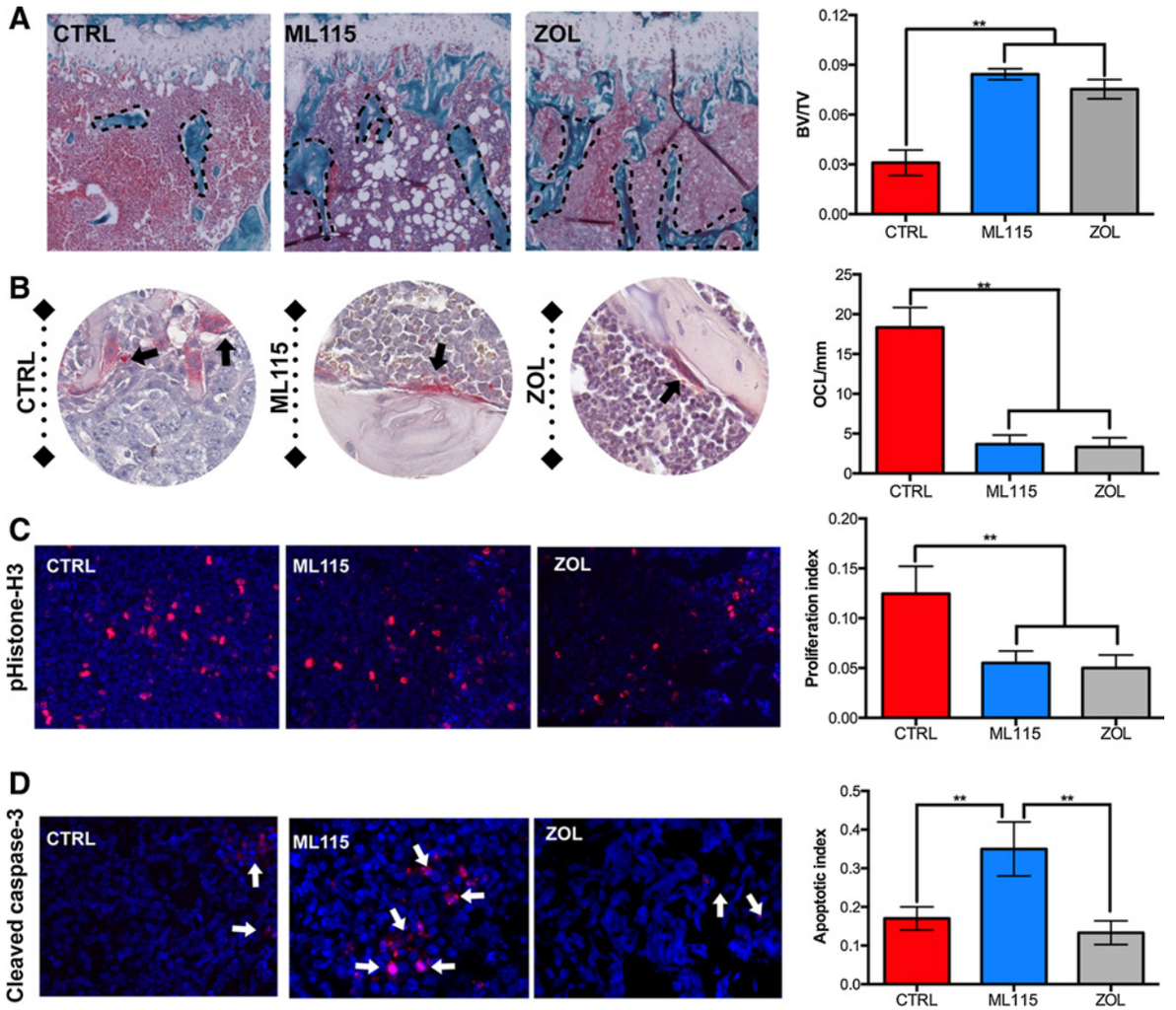

Figure 5.

ML115 protects against cancer-induced osteolysis and promotes tumor apoptosis. **A,** Multiple sections from tumor-bearing limbs in control (CTRL), ML115, and zoledronate (ZOL)-treated groups were generated and trichrome stained. The trabecular bone volume (BV, dashed lines) was measured as a ratio to total volume (TV). **B,** The total number of multinucleated osteoclasts/cells (pink; arrows) per mm of tumor–bone interface was calculated in tissue sections derived from each group. **C** and **D,** The proliferative index [pHistone-H3 positive (red): total number of cells] and apoptotic index [cleaved caspase-3 positive (red, arrows): total number of cells] was calculated for each group. Panels show representative images from the control (CTRL), ML115, and ZOL groups. Asterisks denote statistical significance (**, $P < 0.01$).

remodeling. It is not surprising that MMP activity is often heightened in the context of skeletal malignancies such as bone metastatic cancer and that MMP inhibition has been explored as a means of preventing cancer induced osteolysis in preclinical animal models. For example, broad-spectrum inhibition of MMPs using GM6001 and BB-94 was shown to be an effective strategy in limiting cancer-induced bone destruction and that the inhibition of MMPs could be beneficial when applied in a pre- or post-metastatic therapeutic window (40, 41). In fact, using paralysis/weight loss as a clinical endpoint, administration of GM6001 in a premetastatic context significantly improved overall survival when compared with vehicle alone. More specific MMP inhibitors such as SB-3CT, a covalent mechanism–based inhibitor of the gelatinases MMP-2 and 9, have been shown to significantly reduce cancer growth and associated osteolysis in a model of intraosseous prostate cancer progression (42). While these preclinical studies support the application of MMP inhibitors for the treatment of human skeletal malignancies such as bone metastatic breast and prostate cancer, the reality is that the poor performance of MMP inhibitors in the clinical setting has diminished enthusiasm for the initiation of new clinical trials (43). To successfully translate an MMP inhibitor to the clinic, a number of criteria would have to be met that ideally would include the following characteristics: a clear demonstration for the role of an individual MMP in the progression of a tissue specific cancer/disease, tissue-restricted or cancer cell–specific expression of a target MMP, and the generation of a highly selective inhibitor/antibody that spares the activity of other MMPs with overlapping substrate profiles. We believe that the BMMPIs described here fulfill these criteria.

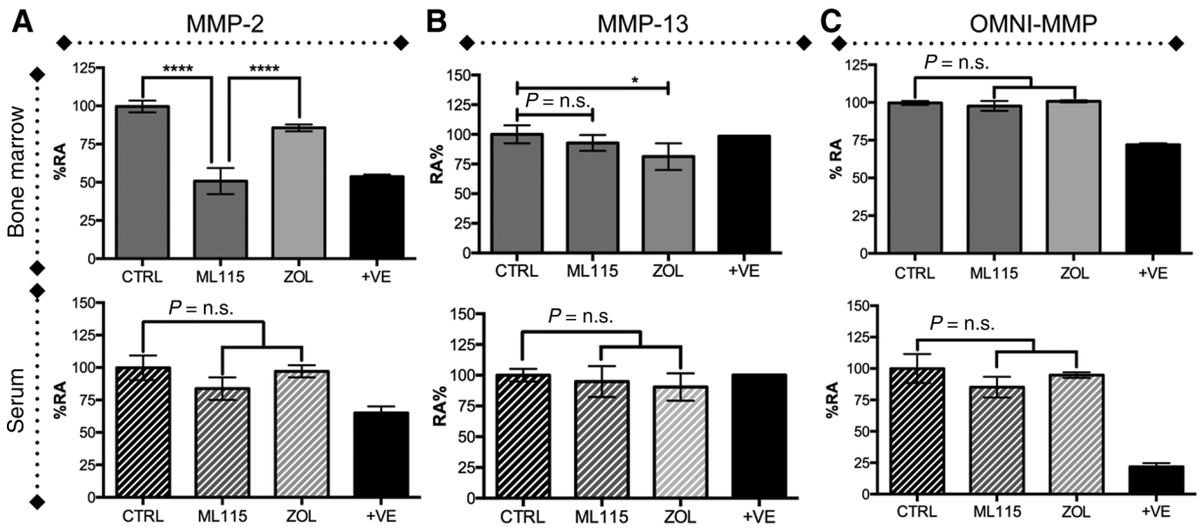

Figure 6.

BMMPIs selectively inhibit MMP-2 activity in the bone marrow microenvironment. **A–C,** Bone marrow supernatants derived from the tumor-bearing limbs of control (CTRL), ML115, and zoledronate (ZOL)-treated groups and matched serum were incubated with an MMP-2–specific (**A**), MMP-13–specific (**B**), or broad-spectrum MMP (OMNI, **C**) activatable fluorogenic peptide for 1 hour at 37°C. Positive indicates positive recombinant MMP control. Asterisks denote statistical significance (*, $P < 0.05$; ****, $P < 0.0001$).

For bone metastatic cancers, we have defined the role of several individual MMPs that are highly expressed at the tumor bone interface including MMP-7 and -9 (44, 45). MMP-2 can be found in both the cancer cell compartment and in the host stroma (11). Cancer cell interaction with bone ECM such as fibronectin via the integrin αvβ6 can induce MMP-2 expression that in turn promotes tumor growth (46). This contribution to cancer cell proliferation is consistent with other studies showing that the forced expression of MMP-2 in cancer cells can significantly accelerate tumor growth in the bone microenvironment (12). Importantly, ablation of MMP-2 in the host compartment also significantly mitigates the *in vivo* growth of PyMT-R221A and 4T1 murine mammary cancers indicating contributory roles for both host and tumor-derived MMP-2 in the progression of the disease (11). Other MMPs have been implicated in skeletal malignancies including MMP-7, 9, 13, and 14 and present potentially alternative therapeutic targets to MMP-2 (10). MMP-7 expression by osteoclasts can process membrane-bound RANKL to yield a soluble form that can accelerate osteoclast formation (45). RANKL can also be processed by other MMPs and members of a disintegrin and metalloproteinase (ADAM) family raising the possibility of compensation in the event of specific inhibition of MMP-7 (45, 47, 48). Ablation of MMP-9, either genetically or pharmacologically, reveals important angiogenic roles for this MMP in vascularization of the bone microenvironment (44, 49). This is primarily because of the ability of MMP-9 to regulate the bioavailability of VEGFA (50). However, ablation of MMP-9 from the host compartment, while limiting angiogenesis, does not inhibit tumor growth (44, 49). This may be, in part, due to the pre-existing sinusoidal and well-vascularized nature of the bone microenvironment. MMP-13, a soluble type I collagenase secreted by mesenchymal stromal cells and osteoblasts, plays roles in bone development (51, 52). The expression of MMP-13 is largely restricted to skeletal tissues and metastatic cancers have been shown to promote the expression and activation of MMP-13 (53). Recently, selective inhibitors of MMP-13 have also proven effective in limiting the progression of bone metastatic breast cancer (54). MMP-14 is a membrane-bound type I collagenase that has been implicated in the invasion and metastasis of several solid cancers (55). Importantly, in bone, MMP-14 is expressed by osteoblasts and osteoclasts and plays a role in bone development and homeostasis (56). Mice null for MMP-14 have severe skeletal phenotypes underscoring the important role for this MMP in bone biology. We would posit that in addition to MMP-2, specific targeting of MMP-13 and or 14 by modifying bisphosphonates might also be an effective treatment for bone metastatic breast cancer. It should also be noted that the strategy of harnessing bisphosphonates to therapeutically target other molecules and reagents to the skeletal tissue has been used by other groups. For example, the coupling of bisphosphonates to osteoprotegerin, a natural RANKL antagonist, should improve selective delivery to bone (57). Covalent conjugation of bisphosphonates with chemotherapies such as 5-fluoro-2′-deoxyuridine (5 FdU) may also improve targeting and efficacy (58).

Musculoskeletal toxicity (MST) was a common adverse event noted in clinical trials for several broad-spectrum MMP inhibitors such as marimastat and, ironically, was indicative of the inhibitors reaching working concentrations (59, 60). MSTs include tendonitis, myalgia, and arthralgia. However, we believe that osteoclast-mediated focal release of MMP-2–selective BMMPIs in the tumor bone microenvironment would limit these side effects. Furthermore, adverse events such as MSTs are rarer with bisphosphonates although other issues such as, osteonecrosis of the jaw, esophageal, and nephrology complications have been noted (61). Whether the grafting of MMP inhibitors to bisphosphonates could heighten the frequency of these side effects remains to be determined. In the current study, we have administered the BMMPIs, ML104, and ML115 at high concentrations (25 mg/kg) and high frequency relative to how bisphosphonates are applied clinically to humans. Even at these high concentrations we noticed no differences in weight loss or behavior between control

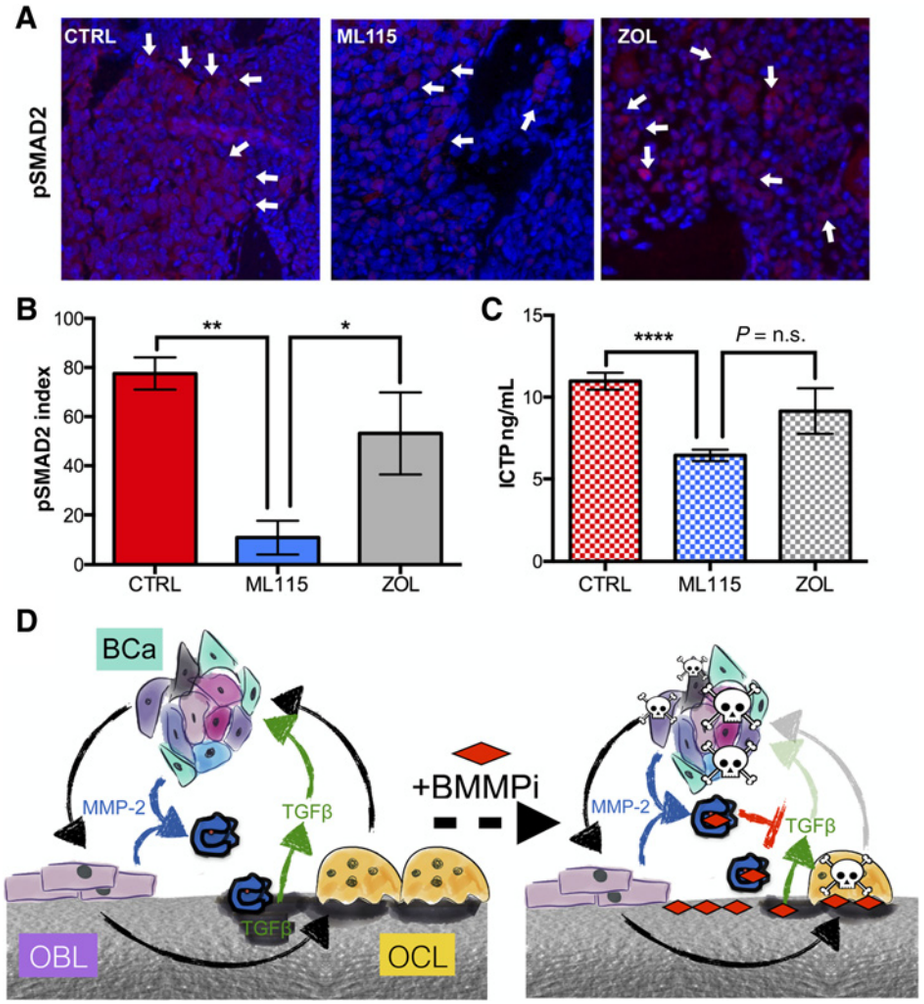

Figure 7.
BMMPI inhibition of MMP-2 substrates in bone metastatic breast cancer. **A** and **B,** The index of pSMAD2 to total cell number in sections derived from vehicle control (CTRL), ML115, and zoledronate (ZOL)-treated groups was calculated. Panels show representative images from each group. Arrows indicate pSMAD2 staining (red). **C,** ICTP ELISA analysis in control, ML115, and zoledronate (ZOL)-treated samples. Asterisks denote statistical significance (*, $P < 0.05$; **, $P < 0.01$; ****, $P < 0.0001$). **D,** Working model of BMMPI action. In the vicious cycle of cancer–bone microenvironment interaction (black arrows), metastatic breast cancer cells promote osteoblasts (OBL) to stimulate osteoclast (OCL) formation. The resultant bone destruction releases growth factors and cytokines that are important for tumor establishment and growth. The expression of MMP-2 (blue enzyme) by the cancer and host compartment not only contributes to type I collagen processing but can regulate TGFβ availability. The addition of MMP-2–selective BMMPIs (signified by red diamond and dashed arrow) that bind to the bone matrix diminishes the ability of osteoclasts to resorb bone and release growth factors while also inhibiting local MMP-2 activity thereby significantly impacting cancer cell survival.

and treatment groups suggesting the BMMPIs are well tolerated (data not shown). Furthermore, our initial biodistribution studies show by LC/MS-MS analysis that ML115 is rapidly cleared from the plasma and accumulates in the bone marrow microenvironment over 24 hours with mice treated over a 3-week period demonstrating a 10-fold higher concentration. We do not anticipate an accumulation of ML115 in other organs. This expectation is based on pharmacodynamic/kinetic studies with unlabeled or radioactively/fluorescently labeled bisphosphonates demonstrating a rapid clearance of the reagents from organs such as the kidneys and livers (62–66). These data, combined with MMP activity assays demonstrate the feasibility of targeting the bone microenvironment with a selective MMP inhibitor.

In conclusion, MMPs are highly expressed in skeletal malignancies such as bone metastatic breast cancer. Genetic ablation and pharmacologic inhibition of MMPs has demonstrated key roles for individual family members such as MMP-2 in the progression of the disease. The translation of specific MMP inhibitors to the clinical setting is difficult in light of previous clinical trial results and the potential for off-target side effects. Here, we have used a novel strategy of applying "bone seeking" MMP-2–selective inhibitors for the treatment of bone metastatic breast cancer and have demonstrated their efficacy *in vivo*. This efficacy is not only due to the ability of the bisphosphonic component of the reagents inhibiting osteoclast function but also via their ability to prevent MMP-2 activation of non-matrix substrates such as TGFβ that are critical mediators of the vicious cycle. We propose that this approach should circumvent potential toxicities associated with systemic MMP-2 inhibition. Given that bisphosphonates are well tolerated in patients, BMMPIs could be quickly translated to the clinical setting where we anticipate they would prevent pathologic fracture but importantly, as opposed to current bisphosphonates, would also extend overall survival for bone metastatic breast cancer patients.

Disclosure of Potential Conflicts of Interest

No potential conflicts of interest were disclosed.

Authors' Contributions

Conception and design: M. Tauro, G. Shay, S.S. Sansil, C.C. Lynch
Development of methodology: M. Tauro, S.S. Sansil, C.C. Lynch
Acquisition of data (provided animals, acquired and managed patients, provided facilities, etc.): M. Tauro, G. Shay, S.S. Sansil
Analysis and interpretation of data (e.g., statistical analysis, biostatistics, computational analysis): M. Tauro, S.S. Sansil, A.M. Neuger, H. Soliman, C.C. Lynch

Writing, review, and/or revision of the manuscript: M. Tauro, S.S. Sansil, A.M. Neuger, H. Soliman, C.C. Lynch
Administrative, technical, or material support (i.e., reporting or organizing data, constructing databases): M. Tauro, A.M. Neuger
Study supervision: M. Tauro, C.C. Lynch
Other (design, synthesis, and characterization of BMMPI compounds): A. Laghezza, M. Tauro, P. Tortorella

Acknowledgments

We would also like to thank Ms. Jeri Francoeur, a Florida Komen Advocate in Science, for her review of the manuscript and excellent contributions.

Grant Support

This research was supported in part by grants NCI-R21CA19198101 (to C.C. Lynch) and the Susan G. Komen Foundation-PDF15332812 (to M. Tauro) made possible through funding from American Airlines. This work was also supported by the Moffitt Translational Research, Microscopy and Small Animal Imaging Cores (P30-CA076292).

The costs of publication of this article were defrayed in part by the payment of page charges. This article must therefore be hereby marked *advertisement* in accordance with 18 U.S.C. Section 1734 solely to indicate this fact.

Received May 17, 2016; revised December 5, 2016; accepted December 7, 2016; published OnlineFirst January 9, 2017.

References

1. Paget S. The distribution of secondary growths in cancer of the breast. Cancer Metastasis Rev 1989;8:98–101.
2. Mundy GR. Metastasis to bone: causes, consequences and therapeutic opportunities. Nat Rev Cancer 2002;2:584–93.
3. Guise TA, Chirgwin JM. Transforming growth factor-beta in osteolytic breast cancer bone metastases 8. Clin Orthop Relat Res 2003: S32–S8.
4. Coleman RE, Major P, Lipton A, Brown JE, Lee KA, Smith M, et al. Predictive value of bone resorption and formation markers in cancer patients with bone metastases receiving the bisphosphonate zoledronic acid. J Clin Oncol 2005;23:4925–35.
5. Puljula E, Turhanen P, Vepsalainen J, Monteil M, Lecouvey M, Weisell J. Structural requirements for bisphosphonate binding on hydroxyapatite: NMR study of bisphosphonate partial esters. ACS Med Chem Lett 2015;6:397–401.
6. Rogers MJ, Crockett JC, Coxon FP, Monkkonen J. Biochemical and molecular mechanisms of action of bisphosphonates. Bone 2011;49:34–41.
7. Lipton A, Fizazi K, Stopeck AT, Henry DH, Brown JE, Yardley DA, et al. Superiority of denosumab to zoledronic acid for prevention of skeletal-related events: a combined analysis of 3 pivotal, randomised, phase 3 trials. Eur J Cancer 2012;48:3082–92.
8. Coleman R, Cameron D, Dodwell D, Bell R, Wilson C, Rathbone E, et al. Adjuvant zoledronic acid in patients with early breast cancer: final efficacy analysis of the AZURE (BIG 01/04) randomised open-label phase 3 trial. Lancet Oncol 2014;15:997–1006.
9. Cook LM, Shay G, Aruajo A, Lynch CC. Integrating new discoveries into the "vicious cycle" paradigm of prostate to bone metastases. Cancer Metastasis Rev 2014;33:511–25.
10. Lynch CC. Matrix metalloproteinases as master regulators of the vicious cycle of bone metastasis. Bone 2011;48:44–53.
11. Thiolloy S, Edwards JR, Fingleton B, Rifkin DB, Matrisian LM, Lynch CC. An osteoblast-derived proteinase controls tumor cell survival via TGF-beta activation in the bone microenvironment. PLoS One 2012;7: e29862.
12. Tester AM, Waltham M, Oh SJ, Bae SN, Bills MM, Walker EC, et al. Pro-matrix metalloproteinase-2 transfection increases orthotopic primary growth and experimental metastasis of MDA-MB-231 human breast cancer cells in nude mice. Cancer Res 2004;64:652–8.
13. Inoue K, Mikuni-Takagaki Y, Oikawa K, Itoh T, Inada M, Noguchi T, et al. A crucial role for matrix metalloproteinase 2 in osteocytic canalicular formation and bone metabolism. J Biol Chem 2006;281: 33814–24.
14. Dallas SL, Rosser JL, Mundy GR, Bonewald LF. Proteolysis of latent transforming growth factor-beta (TGF-beta)-binding protein-1 by osteoclasts. A cellular mechanism for release of TGF-beta from bone matrix. J Biol Chem 2002;277:21352–60.
15. Coussens LM, Fingleton B, Matrisian LM. Matrix metalloproteinase inhibitors and cancer: trials and tribulations. Science 2002;295:2387–92.
16. Tauro M, McGuire J, Lynch CC. New approaches to selectively target cancer-associated matrix metalloproteinase activity. Cancer Metastasis Rev 2014;33:1043–57.
17. Dufour A, Overall CM. Missing the target: matrix metalloproteinase antitargets in inflammation and cancer. Trends Pharmacol Sci 2013; 34:233–42.
18. Rubino MT, Agamennone M, Campestre C, Campiglia P, Cremasco V, Faccio R, et al. Biphenyl sulfonylamino methyl bisphosphonic acids as inhibitors of matrix metalloproteinases and bone resorption. ChemMedChem 2011;6:1258–68.
19. Tauro M, Laghezza A, Loiodice F, Agamennone M, Campestre C, Tortorella P. Arylamino methylene bisphosphonate derivatives as bone seeking matrix metalloproteinase inhibitors. Bioorg Med Chem 2013; 21:6456–65.
20. Madden SF, Clarke C, Gaule P, Aherne ST, O'Donovan N, Clynes M, et al. BreastMark: an integrated approach to mining publicly available transcriptomic datasets relating to breast cancer outcome. Breast Cancer Res 2013;15:R52.
21. Gyorffy B, Lanczky A, Eklund AC, Denkert C, Budczies J, Li Q, et al. An online survival analysis tool to rapidly assess the effect of 22,277 genes on breast cancer prognosis using microarray data of 1,809 patients. Breast Cancer Res Treat 2010;123:725–31.
22. Thiolloy S, Halpern J, Holt GE, Schwartz HS, Mundy GR, Matrisian LM, et al. Osteoclast-derived matrix metalloproteinase-7, but not matrix metalloproteinase-9, contributes to tumor-induced osteolysis. Cancer Res 2009;69:6747–55.
23. Halpern J, Lynch CC, Fleming J, Hamming D, Martin MD, Schwartz HS, et al. The application of a murine bone bioreactor as a model of tumor: bone interaction. Clin Exp Metastasis 2006;23:345–56.
24. Reinhardt S, Zhao M, Mnatsakanyan A, Xu L, Ricklis RM, Chen A, et al. A rapid and sensitive method for determination of veliparib (ABT-888), in human plasma, bone marrow cells and supernatant by using LC/MS/MS. J Pharm Biomed Anal 2010;52:122–8.
25. Sparidans RW, den Hartigh J. Chromatographic analysis of bisphosphonates. Pharm World Sci 1999;21:1–10.
26. Schneider CA, Rasband WS, Eliceiri KW. NIH Image to ImageJ: 25 years of image analysis. Nat Methods 2012;9:671–5.
27. Nakopoulou L, Tsirmpa I, Alexandrou P, Louvrou A, Ampela C, Markaki S, et al. MMP-2 protein in invasive breast cancer and the impact of MMP-2/TIMP-2 phenotype on overall survival. Breast Cancer Res Treat 2003;77: 145–55.
28. Jinga DC, Blidaru A, Condrea I, Ardeleanu C, Dragomir C, Szegli G, et al. MMP-9 and MMP-2 gelatinases and TIMP-1 and TIMP-2 inhibitors in breast cancer: correlations with prognostic factors. J Cell Mol Med 2006; 10:499–510.
29. Talvensaari-Mattila A, Paakko P, Turpeenniemi-Hujanen T. Matrix metalloproteinase-2 (MMP-2) is associated with survival in breast carcinoma. Br J Cancer 2003;89:1270–5.
30. Jezierska A, Motyl T. Matrix metalloproteinase-2 involvement in breast cancer progression: a mini-review. Med Sci Monit 2009;15:RA32–40.
31. Im GI, Qureshi SA, Kenney J, Rubash HE, Shanbhag AS. Osteoblast proliferation and maturation by bisphosphonates. Biomaterials 2004; 25:4105–15.
32. Murakami H, Nakamura T, Tsurukami H, Abe M, Barbier A, Suzuki K. Effects of tiludronate on bone mass, structure, and turnover at the epiphyseal, primary, and secondary spongiosa in the proximal tibia of growing rats after sciatic neurectomy. J Bone Miner Res 1994;9:1355–64.
33. Reginster JY. Oral tiludronate: pharmacological properties and potential usefulness in Paget's disease of bone and osteoporosis. Bone 1992; 13:351–4.

34. Ohnishi H, Nakamura T, Narusawa K, Murakami H, Abe M, Barbier A, et al. Bisphosphonate tiludronate increases bone strength by improving mass and structure in established osteopenia after ovariectomy in rats. Bone 1997;21:335–43.
35. Ory B, Heymann MF, Kamijo A, Gouin F, Heymann D, Redini F. Zoledronic acid suppresses lung metastases and prolongs overall survival of osteosarcoma-bearing mice. Cancer 2005;104:2522–9.
36. Garnero P, Ferreras M, Karsdal MA, Nicamhlaoibh R, Risteli J, Borel O, et al. The type I collagen fragments ICTP and CTX reveal distinct enzymatic pathways of bone collagen degradation. J Bone Miner Res 2003;18:859–67.
37. Benzaid I, Monkkonen H, Stresing V, Bonnelye E, Green J, Monkkonen J, et al. High phosphoantigen levels in bisphosphonate-treated human breast tumors promote Vgamma9Vdelta2 T-cell chemotaxis and cytotoxicity in vivo. Cancer Res 2011;71:4562–72.
38. Garnero P, Borel O, Byrjalsen I, Ferreras M, Drake FH, McQueney MS, et al. The collagenolytic activity of cathepsin K is unique among mammalian proteinases. J Biol Chem 1998;273:32347–52.
39. Delaisse JM, Andersen TL, Engsig MT, Henriksen K, Troen T, Blavier L. Matrix metalloproteinases (MMP) and cathepsin K contribute differently to osteoclastic activities. Microsc Res Tech 2003;61:504–13.
40. Lee J, Weber M, Mejia S, Bone E, Watson P, Orr W. A matrix metalloproteinase inhibitor, batimastat, retards the development of osteolytic bone metastases by MDA-MB-231 human breast cancer cells in Balb C nu/nu mice. Eur J Cancer 2001;37:106–13.
41. Winding B, NicAmhlaoibh R, Misander H, Hoegh-Andersen P, Andersen TL, Holst-Hansen C, et al. Synthetic matrix metalloproteinase inhibitors inhibit growth of established breast cancer osteolytic lesions and prolong survival in mice. Clin Cancer Res 2002; 8:1932–9.
42. Bonfil RD, Sabbota A, Nabha S, Bernardo MM, Dong Z, Meng H, et al. Inhibition of human prostate cancer growth, osteolysis and angiogenesis in a bone metastasis model by a novel mechanism-based selective gelatinase inhibitor. Int J Cancer 2006;118:2721–6.
43. Brinckerhoff CE, Matrisian LM. Matrix metalloproteinases: a tail of a frog that became a prince. Nat Rev Mol Cell Biol 2002;3:207–14.
44. Bruni-Cardoso A, Johnson LC, Vessella RL, Peterson TE, Lynch CC. Osteoclast-derived matrix metalloproteinase-9 directly affects angiogenesis in the prostate tumor-bone microenvironment. Mol Cancer Res 2010;8:459–70.
45. Lynch CC, Hikosaka A, Acuff HB, Martin MD, Kawai N, Singh RK, et al. MMP-7 promotes prostate cancer-induced osteolysis via the solubilization of RANKL. Cancer Cell 2005;7:485–96.
46. Dutta A, Li J, Lu H, Akech J, Pratap J, Wang T, et al. Integrin alphavbeta6 promotes an osteolytic program in cancer cells by upregulating MMP2. Cancer Res 2014;74:1598–608.
47. Lum L, Wong BR, Josien R, Becherer JD, Erdjument-Bromage H, Schlondorff J, et al. Evidence for a role of a tumor necrosis factor-alpha (TNF-alpha)-converting enzyme-like protease in shedding of TRANCE, a TNF family member involved in osteoclastogenesis and dendritic cell survival. J Biol Chem 1999;274:13613–8.
48. Schlondorff J, Lum L, Blobel CP. Biochemical and pharmacological criteria define two shedding activities for TRANCE/OPGL that are distinct from the tumor necrosis factor alpha convertase. J Biol Chem 2001;276:14665–74.
49. Nabha SM, Bonfil RD, Yamamoto HA, Belizi A, Wiesner C, Dong Z, et al. Host matrix metalloproteinase-9 contributes to tumor vascularization without affecting tumor growth in a model of prostate cancer bone metastasis. Clin Exp Metastasis 2006;23:335–44.
50. Bergers G, Brekken R, McMahon G, Vu TH, Itoh T, Tamaki K, et al. Matrix metalloproteinase-9 triggers the angiogenic switch during carcinogenesis. Nat Cell Biol 2000;2:737–44.
51. Stickens D, Behonick DJ, Ortega N, Heyer B, Hartenstein B, Yu Y, et al. Altered endochondral bone development in matrix metalloproteinase 13-deficient mice 2. Development 2004;131:5883–95.
52. Inada M, Wang Y, Byrne MH, Rahman MU, Miyaura C, Lopez-Otin C, et al. Critical roles for collagenase-3 (Mmp13) in development of growth plate cartilage and in endochondral ossification. Proc Natl Acad Sci U S A 2004;101:17192–7.
53. Morrison C, Mancini S, Cipollone J, Kappelhoff R, Roskelley C, Overall C. Microarray and proteomic analysis of breast cancer cell and osteoblast co-cultures: role of osteoblast matrix metalloproteinase (MMP)-13 in bone metastasis. J Biol Chem 2011;286:34271–85.
54. Shah M, Huang D, Blick T, Connor A, Reiter LA, Hardink JR, et al. An MMP13-selective inhibitor delays primary tumor growth and the onset of tumor-associated osteolytic lesions in experimental models of breast cancer. PLoS One 2012;7:e29615.
55. Rowe RG, Weiss SJ. Navigating ECM barriers at the invasive front: the cancer cell-stroma interface. Annu Rev Cell Dev Biol 2009;25:567–95.
56. Holmbeck K, Bianco P, Pidoux I, Inoue S, Billinghurst RC, Wu W, et al. The metalloproteinase MT1-MMP is required for normal development and maintenance of osteocyte processes in bone. J Cell Sci 2005;118:147–56.
57. Doschak MR, Kucharski CM, Wright JE, Zernicke RF, Uludag H. Improved bone delivery of osteoprotegerin by bisphosphonate conjugation in a rat model of osteoarthritis. Mol Pharm 2009;6:634–40.
58. Schott S, Vallet S, Tower RJ, Noor S, Tiwari S, Schem C, et al. In vitro and in vivo toxicity of 5-FdU-alendronate, a novel cytotoxic bone-seeking duplex drug against bone metastasis. Invest New Drugs 2015;33:816–26.
59. Sparano JA, Bernardo P, Stephenson P, Gradishar WJ, Ingle JN, Zucker S, et al. Randomized phase III trial of marimastat versus placebo in patients with metastatic breast cancer who have responding or stable disease after first-line chemotherapy: Eastern Cooperative Oncology Group trial E2196. J Clin Oncol 2004;22:4683–90.
60. Krzeski P, Buckland-Wright C, Balint G, Cline GA, Stoner K, Lyon R, et al. Development of musculoskeletal toxicity without clear benefit after administration of PG-116800, a matrix metalloproteinase inhibitor, to patients with knee osteoarthritis: a randomized, 12-month, double-blind, placebo-controlled study. Arthritis Res Ther 2007;9:R109.
61. Rogers MJ, Watts DJ, Russell RG. Overview of bisphosphonates. Cancer 1997;80:1652–60.
62. Lin JH, Lu AY. Role of pharmacokinetics and metabolism in drug discovery and development. Pharmacol Rev 1997;49:403–49.
63. Skvortsov VG, Stepanenko VF, Petriev VM, Orlov M, Kriukova IG, Sokolov VA, et al. [Pharmacokinetic and dosimetric characteristics of new radiopharmaceutical based on complexes of 103Pd and albumin microspheres]. Radiats Biol Radioecol 2010;50:703–11.
64. Bahrami-Samani A, Anvari A, Jalilian AR, Shirvani-Arani S, Yousefnia H, Aghamiri MR, et al. Production, quality control and pharmacokinetic studies of (177)Lu-EDTMP for human bone pain palliation therapy trials. Iran J Pharm Res 2012;11:137–44.
65. Roelofs AJ, Coxon FP, Ebetino FH, Lundy MW, Henneman ZJ, Nancollas GH, et al. Fluorescent risedronate analogues reveal bisphosphonate uptake by bone marrow monocytes and localization around osteocytes in vivo. J Bone Miner Res 2010;25:606–16.
66. Roelofs AJ, Stewart CA, Sun S, Blazewska KM, Kashemirov BA, McKenna CE, et al. Influence of bone affinity on the skeletal distribution of fluorescently labeled bisphosphonates in vivo. J Bone Miner Res 2012;27:835–47.